

A fully automatic method for image rectification of AVHRR satellite data

André R. S. Marçal, Janete Borges

Faculdade de Ciências, Universidade do Porto
Portugal

Abstract - Most remote sensing applications require the geometric distortions present on satellite images to be corrected. The geometric correction methods usually need the identification of ground control points, which is a time consuming task and requires human intervention. The method proposed here intends to automate this stage by using image matching techniques. The satellite images are first segmented into water, land and cloud. The matching is performed using a library of search points alongside the coastline. The matching is done 5 times for each search point, using target matrices of various dimensions. The method was tested on 10 AVHRR images and the results are presented and discussed.

I. INTRODUCTION

Remote sensing satellites acquire huge amounts of data from the surface and atmosphere of the Earth every day. Most of the data is transmitted to ground stations and stored in archives for subsequent processing. However, for some environmental monitoring applications, a fast chain of processing is required in order for the satellite data to be useful. This type of applications require frequent global coverage, which is possible for low spatial resolution sensors on polar orbital satellites, such as AVHRR and SeaWiFS. The AVHRR instrument has 5 spectral bands, ranging from the visible to the thermal infrared region. The AVHRR spatial resolution is 1.1 km at nadir, and its wide swath (2800km) allows for complete Earth coverage every day [1]. The data is delivered by some satellite stations (e.g. The University of Dundee satellite station) only a few minutes after the satellite pass. However, as the raw data collected by the satellite radiometer is not suitable for most monitoring purposes, a number of processing steps ought to be made on the original satellite data before the required piece of information can be obtained. These can include image calibration, additional image production, image classification, geometric correction and image registration. Some of these tasks can be easily automated. However, to obtain geometrically corrected images with pixel size precision, human intervention is usually required [2]. The method presented here intends to remove the intervention

of an operator allowing for fully automatic image registration of AVHRR data.

II. GEOMETRIC CORRECTION METHODS

There are several methods for correcting the geometric distortions present on satellite images. The geometric correction methods can be divided into three groups: (i) modeling the nature and magnitude of the sources of distortion, using these models to establish a correction formulae [3]; (ii) empirical, using Ground Control Points (GCPs) –points identified on the image whose geographic coordinates are known; (iii) mixed, using both methods (i) and (ii). Methods of type (i) are very effective in that they can be automated. However, its precision is constrained on the exact knowledge of the satellite orbit and the sensors attitude. In the case of AVHRR there are uncertainties of around 0.1 degrees in roll pitch and yaw [4]. The methods of type (ii) can theoretically provide good quality geometrically corrected satellite images. However, this requires that a large number of well spread GCPs are available, as high order transformation functions need to be used. This is an obvious limitation as the identification of GCPs is a time consuming task. Furthermore, the number of places where it is possible to identify GCPs is quite often small due to the characteristics of the study area and to cloud cover. The methods of type (iii) are generally the most effective in that they provide an initial automatic image correction which is further improved by the use of a GCP based transformation. Several such methods were used to correct AVHRR data, for example [5] and [6]. It is worth pointing that the precision of these methods is varied and that they all require the identification of at least one GCP.

There have been some attempts to fully automate the geometric correction of AVHRR data. Mao et al developed a method based on coastline extraction and matching [7]. Their method is based on a correlation-relaxation technique and is suitable in areas where large cloud free areas of the coastline are available [7].

III. FULLY AUTOMATIC GEOMETRIC CORRECTION METHOD

The fully automatic method proposed here for the geometric correction of satellite images, collected by the AVHRR sensor, involves 4 stages:

- (A) an initial image transformation (f) of the *original* AVHRR image, based on orbital parameters, creating a geo-referenced image (*auto*).
- (B) image segmentation of the *auto* image created into 4 classes (land, water, cloud and mixed water + land).
- (C) automatic GCP collection, by image matching, and establishment of a transformation function (g) for the image *auto*.
- (D) *final* image production, obtained directly from the *original* image, combining both image transformation functions f and g .

A. Initial image transformation (f)

The initial image transformation is a third order polynomial function, which is derived using a simplified orbital model [5]. This is an automatic task, requiring a number of satellite orbital parameters which are provided with the image data [2]. This geometric correction accounts for distortions due to the Earth curvature and rotation and, to a certain degree, the satellite velocity and sensor orientation. However, the internal recorded time and the AVHRR attitude are not precisely known, which can account for an error of several kilometers in the estimated coordinates of any given pixel in the original image. The *auto* image produced has a low frequency error of several kilometres both in X and Y coordinates, and a high frequency error typically of 1 to 2 km [6].

B. Image segmentation

The images produced by (A) can be used to identify GCPs by an operator. However, trying to use matching techniques directly on these satellite images would most likely not work due to the large variability of the recorded signal from the same location on images from different dates. The main reason for this is the atmosphere composition, highly variable both temporally and spatially, which strongly influences the recorded signal.

A more efficient approach is to make an image segmentation into a small number of classes. The segmentation process aims at discriminating between water/land and cloud/clear. This could be recorded in 2 bitmap images. Instead we use 8 bit images with water pixels assigned to 0, land pixels to 10 and cloudy pixels to 255. Mixed water/land pixels are assigned the value 5. An additional improvement would be to have levels between 1 and 9 assigned to mixed water/land pixels at various proportions.

C. Second image transformation (g)

As mentioned the *auto* image requires an additional transformation. A first order polynomial transformation function is generally sufficient to reduce the error to sub pixel level [6]. A number of GCPs is used to obtain the function g by the least squares method. The GCPs are obtained by image matching methods, described in detail in section IV.

D. Final image generation

The transformation functions f and g are combined to obtain a third order polynomial function. This function is used to produce the *final* geometrically corrected imagery directly from the *original* imagery. This prevents excessive smoothing due to multiple image resampling.

IV. AUTOMATIC “GCP” DETECTION ON AVHRR IMAGES

A reference image was produced for the west part of the Iberian Peninsula using the lat/long coordinate system. An image of 300 by 800 pixels of 1 km² each was created. Each pixel has a value between 0 (100% water) and 10 (0% water). Mixed water/land pixels have values between 1 and 9. For example a 1 km² pixel with 30 % water will have a value of 7. This reference image was produced by Vector to Raster conversion of a 100m resolution vector database with coastline and political boundaries [8]. A detail of the reference image with the vector data overlaid (red) is presented on Figure 1. The numerical values of mixed pixels are also overlaid (blue). The area featured is in the southwest of Portugal, around Sagres.

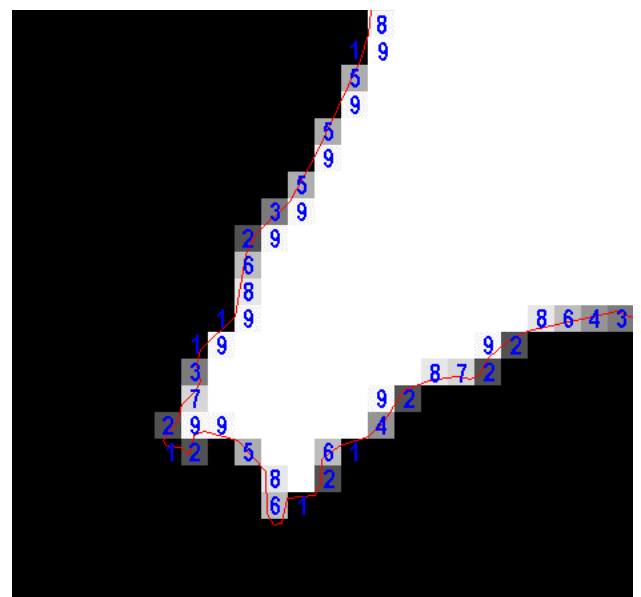


Fig. 1 - Section of the reference image.



Fig. 2 - Location of the 30 Search Points (SPs) used.

A number of suitable Search Points (SPs) were identified on the reference image. These were chosen in areas such as capes, peninsulas or other well distinct areas alongside the coastline. A total of 30 SPs were selected for the test area presented here. Their location and distribution can be seen on Figure 2.

A target matrix size of 5 by 5 is initially set for the first SP. A search matrix of 21 by 21 is used, centered on the same location on the segmented *auto* image. If there are pixels contaminated by cloud on the search matrix the SP is rejected. Otherwise, the maximum correlation between the search and target matrices is looked for. The correlation (r)

between 2 matrices of the same dimension is given by Equation 1, where g_1 is the target matrix, g_2 the search sub-matrix, and $\langle g_1 \rangle$ and $\langle g_2 \rangle$ are corresponding arithmetic means of the densities [9]. This equation was adapted for the two dimensional case. The maximum correlation between the target matrix and all the sub-matrices of the same size in the search area, will correspond to the best match. The SP coordinates and the the best match centre X,Y coordinates in the *auto* image are, at this stage, considered to be a GCP.

$$\text{Eq. 1} \quad r = \frac{\sum (g_1 - \langle g_1 \rangle)(g_2 - \langle g_2 \rangle)}{\sqrt{\sum (g_1 - \langle g_1 \rangle)^2 \sum (g_2 - \langle g_2 \rangle)^2}}$$

The process is repeated for the same SP, increasing the target matrix to 7 by 7 pixels. The result will be a second estimation for that GCP. This is then repeated 3 more times, with target matrices of 9 by 9, 11 by 11 and 13 by 13. The search matrix is also increased, to 31 by 31, 41 by 41 and 41 by 41 respectively. Assuming there are no cloudy pixels, 5 possible X,Y values for the SP are now available to establish a GCP. In theory the results from the various matching attempts should only vary by a pixel or so. However, due to similarities in the coastline, it often happens that the best match is not on the right location. This is more likely to happen for large search matrices. The final X,Y values are obtained as an average of the estimate values which do not lie further than 2 pixels away from the median X,Y value estimates. These final X,Y values and the SP coordinates form a GCP.

The procedure described above is repeated for all the SPs. The number of valid GCPs will depend on the presence of cloud and a rejection criteria which will reject the point if more than 50% of estimates are wrong. A polynomial transformation function (g) in the X and Y coordinates is established between the *auto* image and the *final* georeferenced image. This function can be either 1st order or 0 order (a simple translation).

A 3rd order polynomial transformation function is applied to the *original* satellite image, which is a modification of functions f by the polynomial transformation g .

V. RESULTS

Ten AVHRR images, from the NOAA 14 satellite, were selected to test the geometric correction method proposed. The images are all from August 1995, covering the west part of the Iberian Peninsula. This set of data was chosen because the images were acquired with various viewing angles, and most have extensive cloudy areas.

The shape of the image after the initial image transformation is nearly the same as a rectified image, except for an offset of several pixels in both E-W and N-S directions. This offset was from 0 to 5 km E-W and from 7 to 27 km N-S in the images tested.

Due to the amount of cloudy areas the number of valid matches varied between 8 and 25 from a total of 30 SPs

searched. Final georeferenced images were produced for the 10 images teste. The 100m resolution vector database with coastline and political boundaries was overlaid on these *final* images. A verification of the quality of the georeferenced images was made by visual inspection. The results were considered good. Figure 3 shows a detail of the final georeferenced image from the 5th of August, with the 100m coastline vector data overlaid. This is a RGB colour composite from AVHRR bands 1 (visible - red), 2 (near infrared) and 5 (thermal infrared), where the land areas are well distinguishable from sea and cloud.

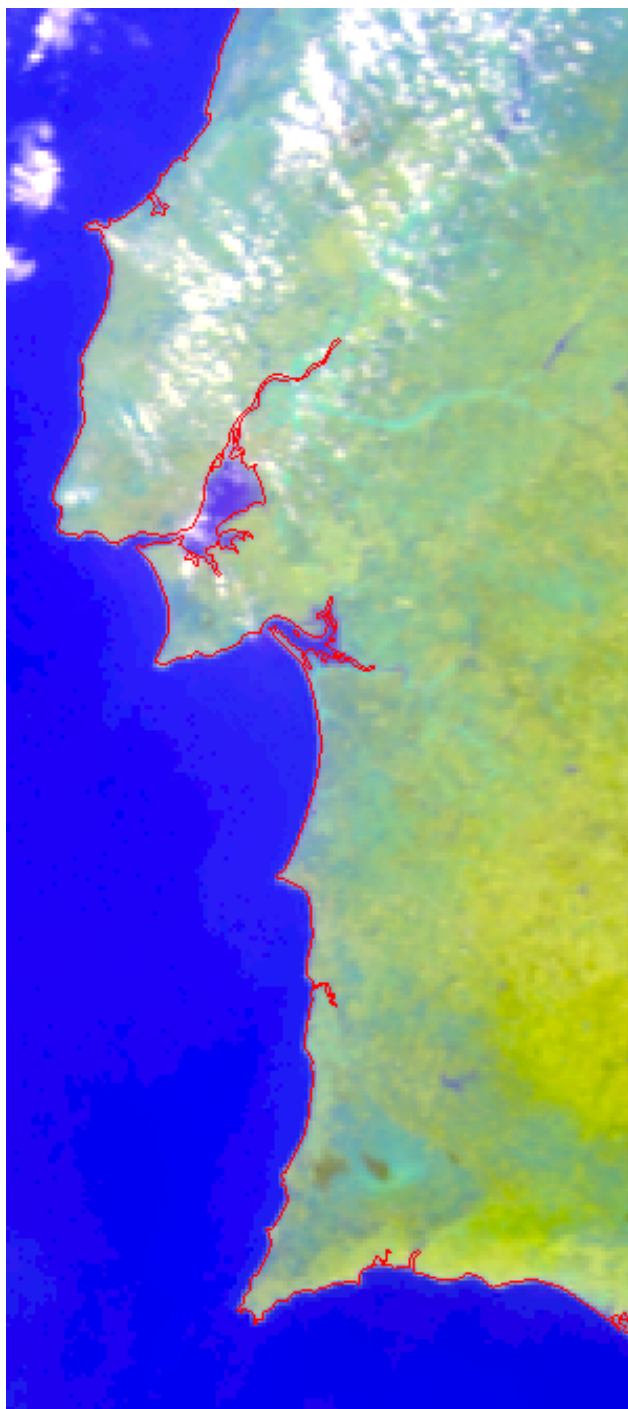


Fig. 3 - Example of automatic georeferenced image.

VI. CONCLUSIONS

There is obvious interest in having fully automatic methods for the geometric correction of satellite images. This is mostly important for sensors such as the AVHRR where the data is distributed shortly after the image acquisition, allowing for near real time monitoring. The most suitable methods for the geometric correction of these images involve an initial automatic correction, based on orbital parameters, followed by a low order transformation to account for residual errors. The image matching method proposed here proved to be effective for establishing this complementary image correction, without the manual identification of GCPs.

The major source of error for this method was due to similarities within the coastline, which induce incorrect GCPs to be selected. Another likely source of error is during the segmentation stage. More work on this topic is under way. Better decision criteria are currently being established for rejecting estimate GCPs, GCPs from the regression, and ultimately the whole image. Plans for future work also include the adaptation of the matching algorithms to incorporate sub-pixel accuracy.

ACKNOWLEDGMENTS

This work was done within the SADMOS project, financed by the FCT / POCTI. The authors also wish to thank the NERC Dundee Satellite Receiving Station for providing the AVHRR data (www.sat.dundee.ac.uk).

REFERENCES

- [1] Cracknell, A. P., 1997, The Advanced Very High Resolution Radiometer, Taylor & Francis
- [2] Marçal, A. R. S., Slater, M. T., 1997, A system for near real time processing of NOAA-AVHRR satellite data: application to snow monitoring in Scotland, "Proceedings of the Sixth International Conference on Image processing and its Applications", Dublin, Ireland, 14-17 July 1997, 546-55
- [3] Richards, J. A., Xiuping, J., 1999, Remote Sensing Digital Image Analysis, Springer
- [4] Brush, R.J.H., 1985, A method for Real-Time Navigation of AVHRR Imagery, "IEEE Transactions on Geoscience and Remote Sensing", Vol. GE-23, No. 6, 876-887
- [5] Ho, D., Asem, A., 1986, NOAA AVHRR image referencing, "International Journal of Remote Sensing", Vol. 7, No. 7, 895-904
- [6] Marçal, A.R.S., 1999, A new method for high accuracy navigation of NOAA AVHRR imagery, "International Journal of Remote Sensing", Vol. 20, No. 17, 3273-3280
- [7] Mao, Z., Pan, D., Huang, H., Huang, W., 2001, Automatic registration of SeaWiFS and AVHRR imagery, "International Journal of Remote Sensing", Vol. 22, No. 9, 1725-1735
- [8] ESRI, 1995, European Countries Data Set, www.esri.com
- [9] Kraus, K., 1993, Photogrammetry – Fundamentals and Standard Processes, Dümmler / Bonn